

Nuclear Matter Equation of State

James M. Lattimer

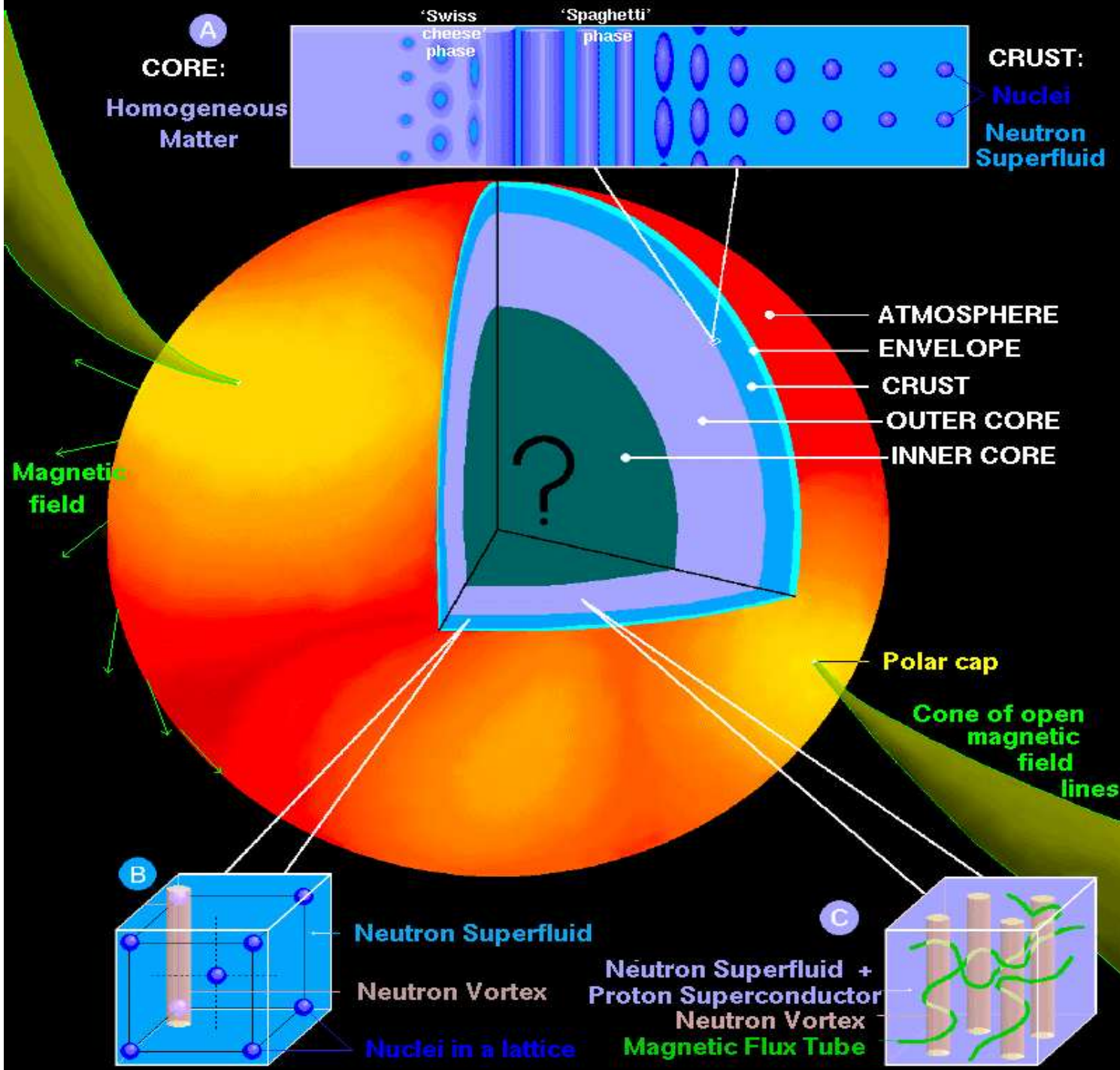
`lattimer@astro.sunysb.edu`

Department of Physics & Astronomy
Stony Brook University

Neutron Stars and the Equation of State

- Extreme Properties
- Pulsar Constraints – Rotation and Mass
- Pressure–Radius Correlation and the Nuclear Symmetry Energy
- Observational Mass and Radius Constraints
- Gravitational Radiation and Tidal Love Numbers

A NEUTRON STAR: SURFACE and INTERIOR



Credit: Dany Page, UNAM

Relevant Observations

- Maximum and Minimum Mass (Binary Pulsars)
- Minimum Rotational Period
- Radiation Radii or Redshifts from X-ray Thermal Emission
- Crustal Cooling Timescale from X-ray Transients
- X-ray Bursts from Accreting Neutron Stars
- Seismology from Giant Flares from Magnetars
- Pulsar Glitches
- Long-Term Neutron Star Cooling (URCA or not)
- Moments of Inertia from Spin-Orbit Coupling
- Neutrinos from Proto-Neutron Stars (Binding Energies, Neutrino Opacities, Radii)
- Redshifts from Pulse Shape Modulation
- Gravitational Radiation from Mergers (Masses from Inspiral, Radii from Tides)

Neutron Star Structure

Tolman-Oppenheimer-Volkov equations of relativistic hydrostatic equilibrium:

$$\frac{dp}{dr} = -\frac{G}{c^2} \frac{(m + 4\pi pr^3)(\epsilon + p)}{r(r - 2Gm/c^2)}$$
$$\frac{dm c^2}{dr} = 4\pi \epsilon r^2$$

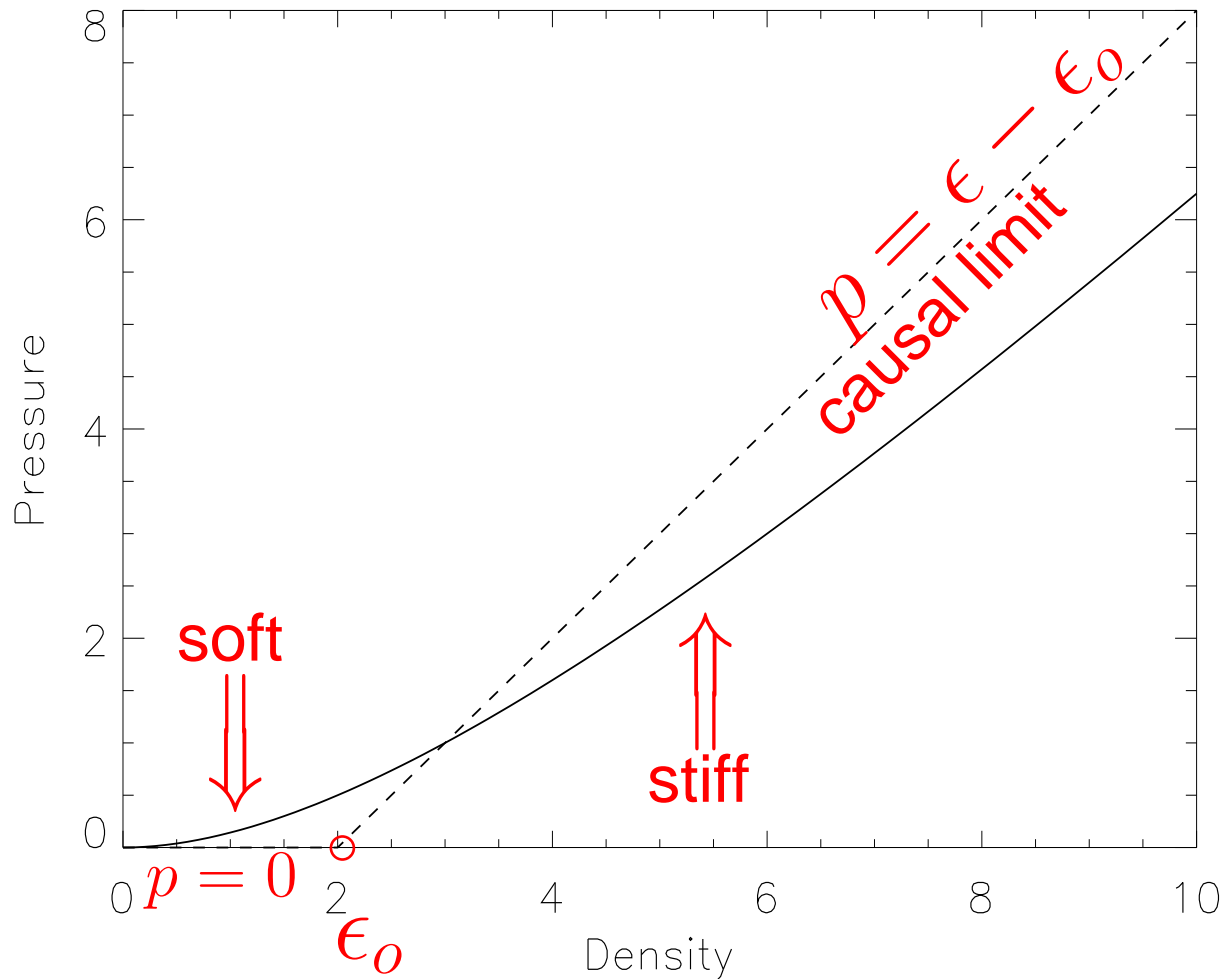
p is pressure, ϵ is mass-energy density

Useful analytic solutions exist:

- Uniform density $\epsilon = \text{constant}$
- Tolman VII $\epsilon = \epsilon_c [1 - (r/R)^2]$
- Buchdahl $\epsilon = \sqrt{pp_*} - 5p$
- Tolman IV $\nu(r) = \nu(0) + N \ln [1 + (r/a)^2]$

Extreme Properties of Neutron Stars

- The most compact configurations occur when the low-density equation of state is "soft" and the high-density equation of state is "stiff".



ϵ_0 is the only EOS parameter

The TOV solutions scale with ϵ_0

Maximum Mass, Minimum Period

Theoretical limits from GR and causality

- $M_{max} = 4.2(\epsilon_s/\epsilon_0)^{1/2} M_\odot$

Rhoades & Ruffini (1974), Hartle (1978)

- $R_{min} = 2.9GM/c^2 = 4.3(M/M_\odot) \text{ km}$

Lindblom (1984), Glendenning (1992), Koranda, Stergioulas & Friedman (1997)

- $\epsilon_c < 4.5 \times 10^{15} (M_\odot/M_{largest})^2 \text{ g cm}^{-3}$

Lattimer & Prakash (2005)

- $P_{min} \simeq (0.74 \pm 0.03)(M_\odot/M_{sph})^{1/2} (R_{sph}/10 \text{ km})^{3/2} \text{ ms}$

Koranda, Stergioulas & Friedman (1997)

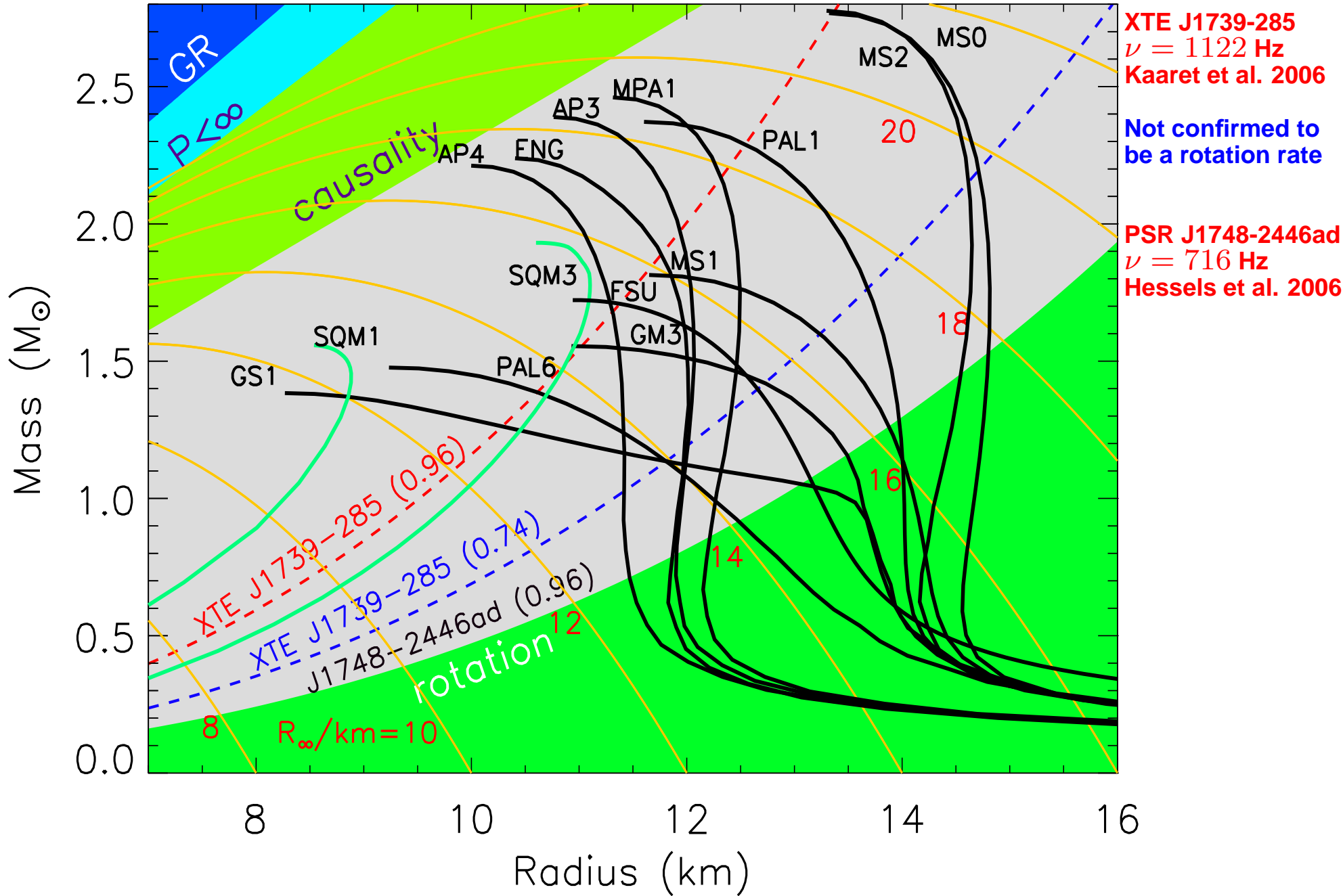
- $P_{min} \simeq 0.96(M_\odot/M_{sph})^{1/2} (R_{sph}/10 \text{ km})^{3/2} \text{ ms}$ (empirical)

Lattimer & Prakash (2004)

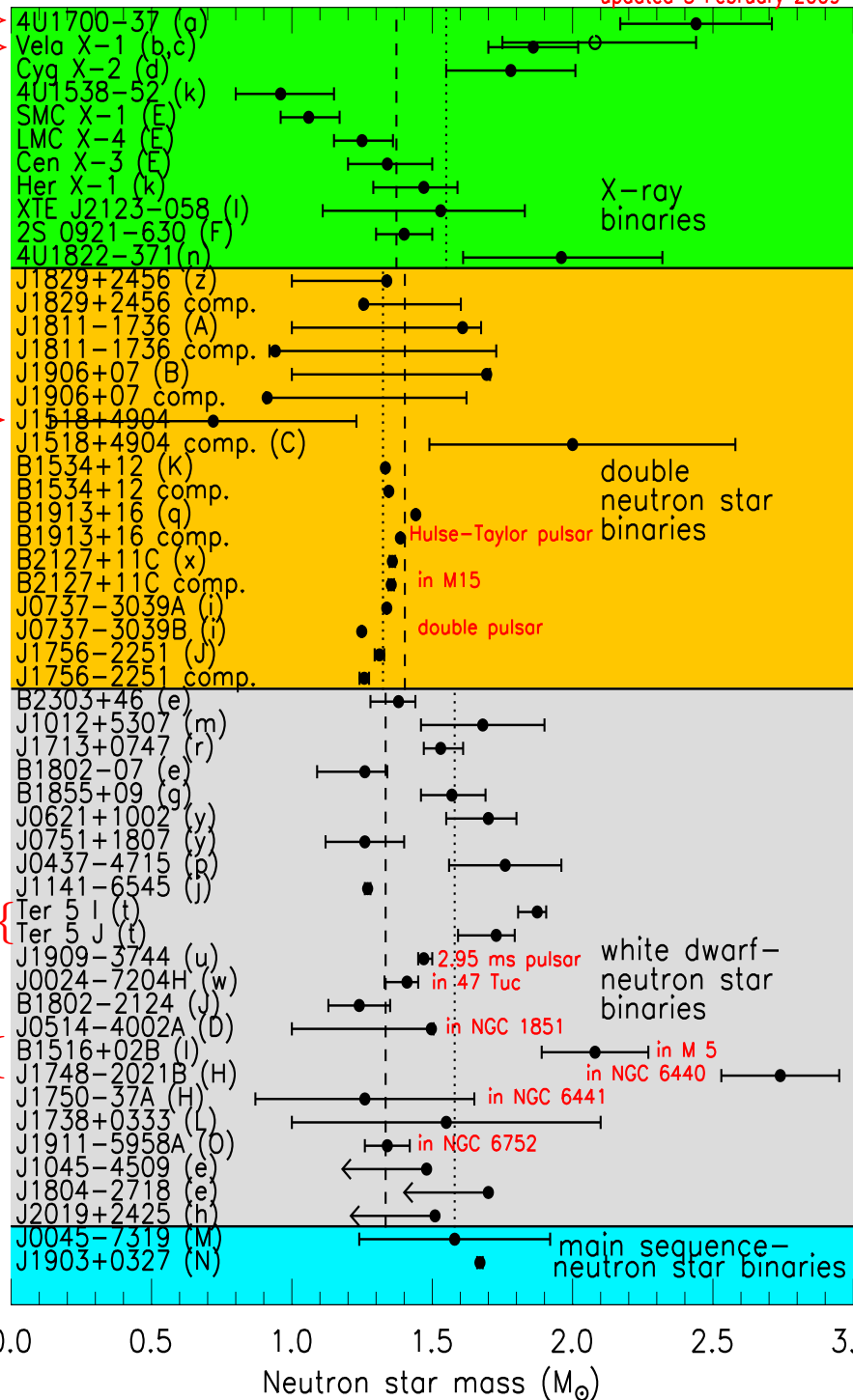
- $\epsilon_c > 0.91 \times 10^{15} (1 \text{ ms}/P_{min})^2 \text{ g cm}^{-3}$ (empirical)

- $cJ/GM^2 \lesssim 0.5$ (empirical, neutron star)

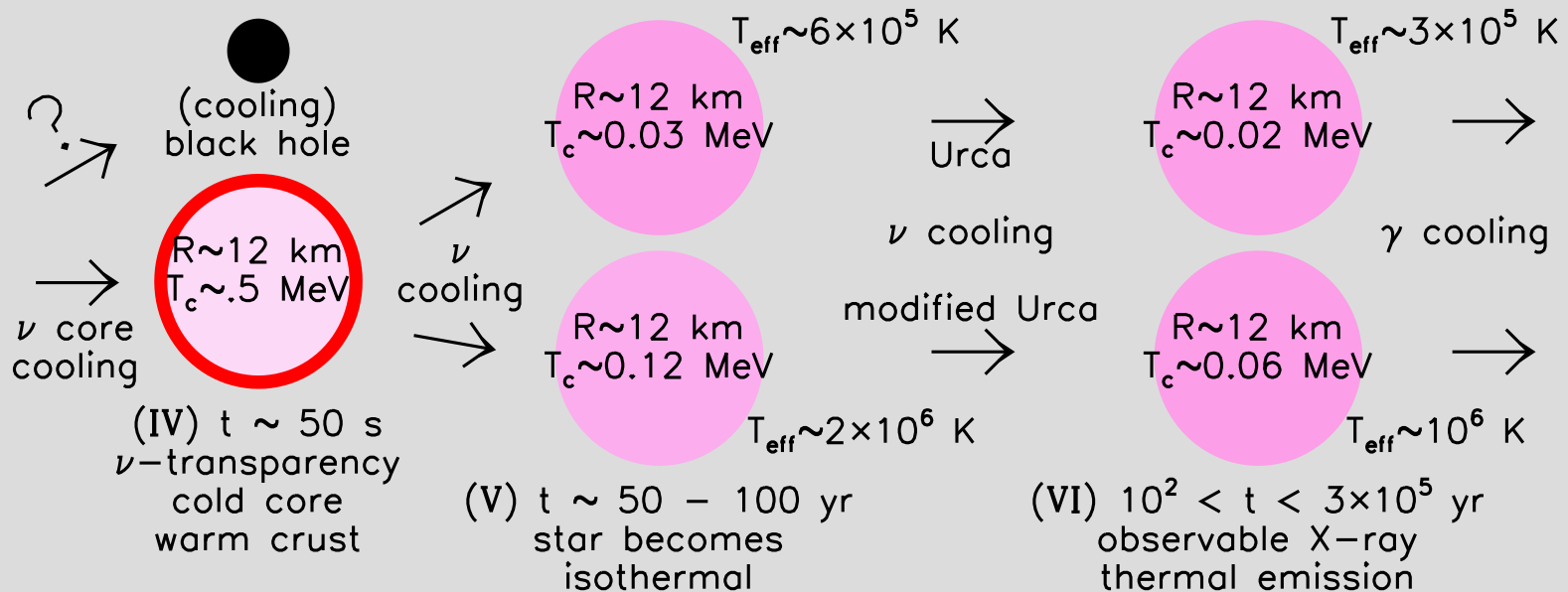
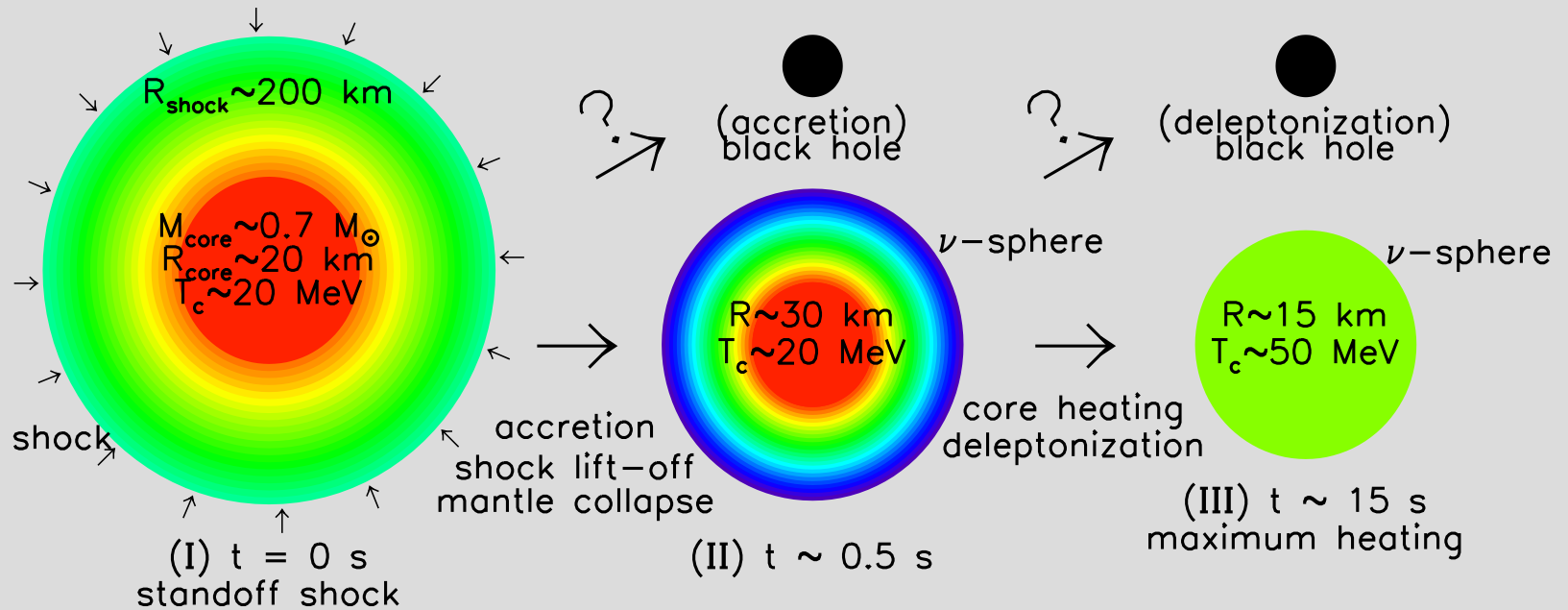
Constraints from Pulsar Spins



Black hole? ⇒
Firm lower mass limit? ⇒

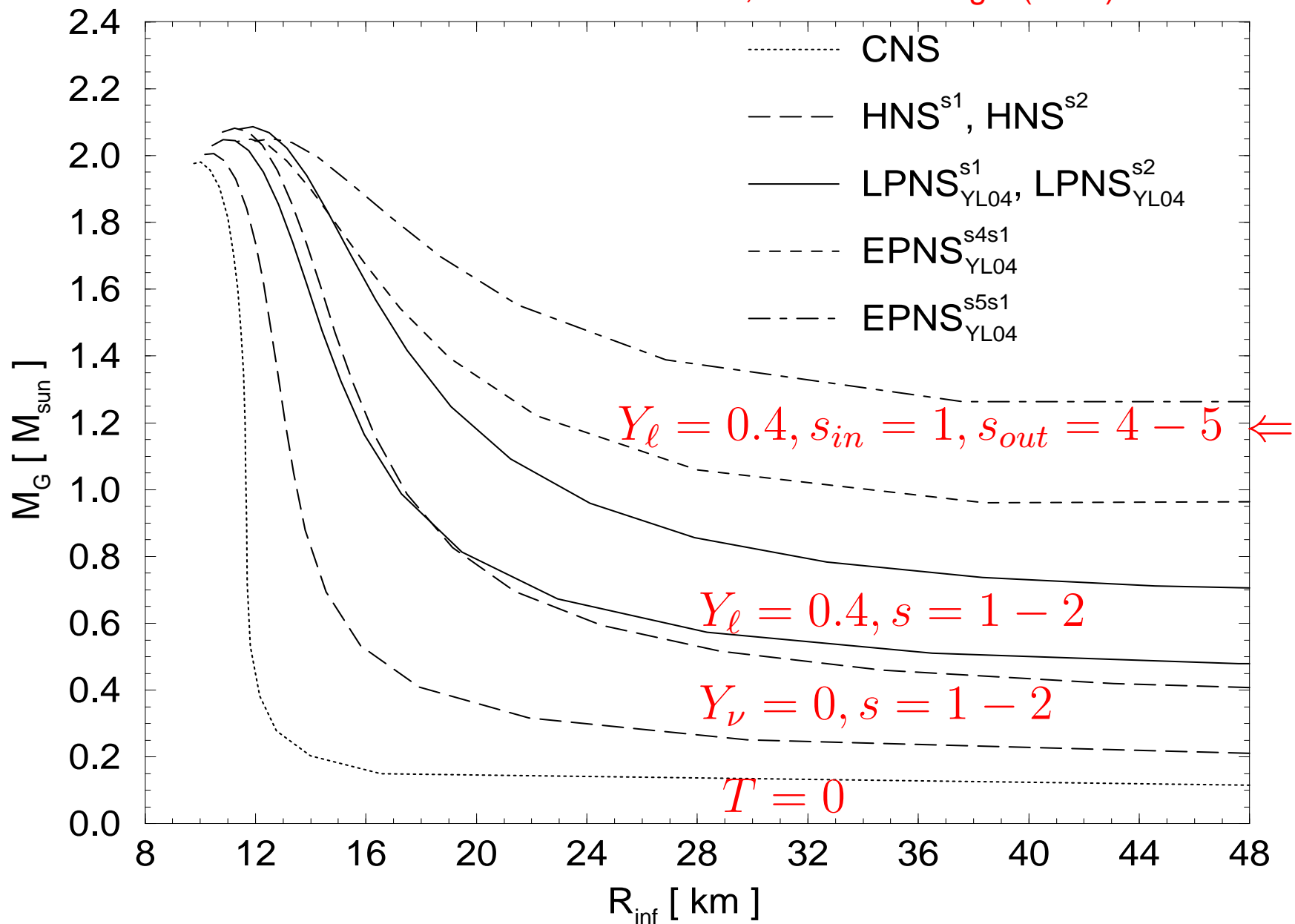


Proto-Neutron Stars



Effective Minimum Masses

Strobel, Schaab & Weigel (1999)



Neutron Star Matter Pressure and the Radius

$$p \simeq K \epsilon^{1+1/n}$$

$$n^{-1} = d \ln p / d \ln \epsilon - 1 \sim 1$$

$$R \propto K^{n/(3-n)} M^{(1-n)/(3-n)}$$

$$R \propto p_*^{1/2} \epsilon_*^{-1} M^0$$

$$(1 < \epsilon_*/\epsilon_0 < 2)$$

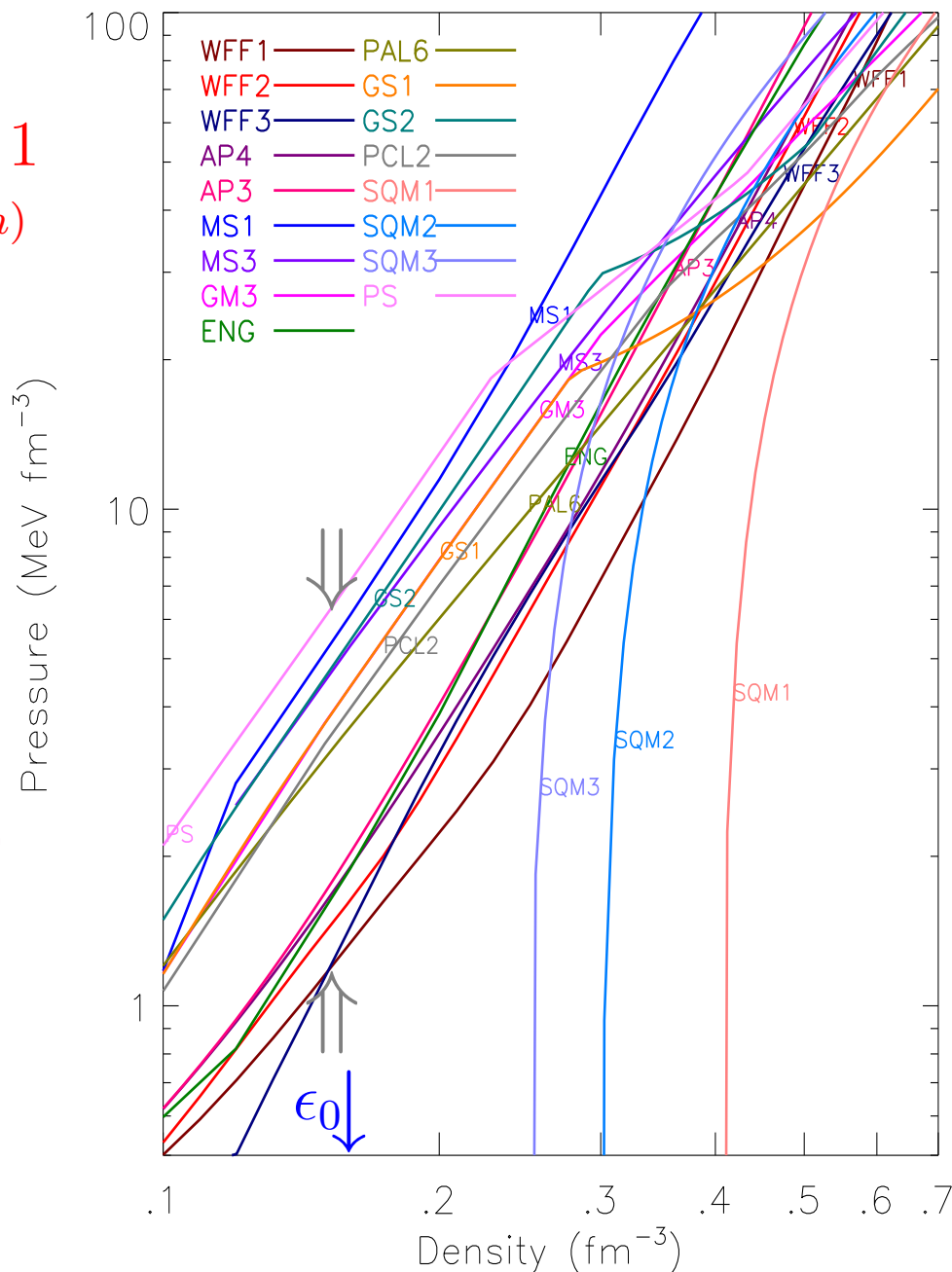
Wide variation:

$$1.2 < \frac{p(\epsilon_0)}{\text{MeV fm}^{-3}} < 7$$

GR phenomenological result (Lattimer & Prakash 2001)

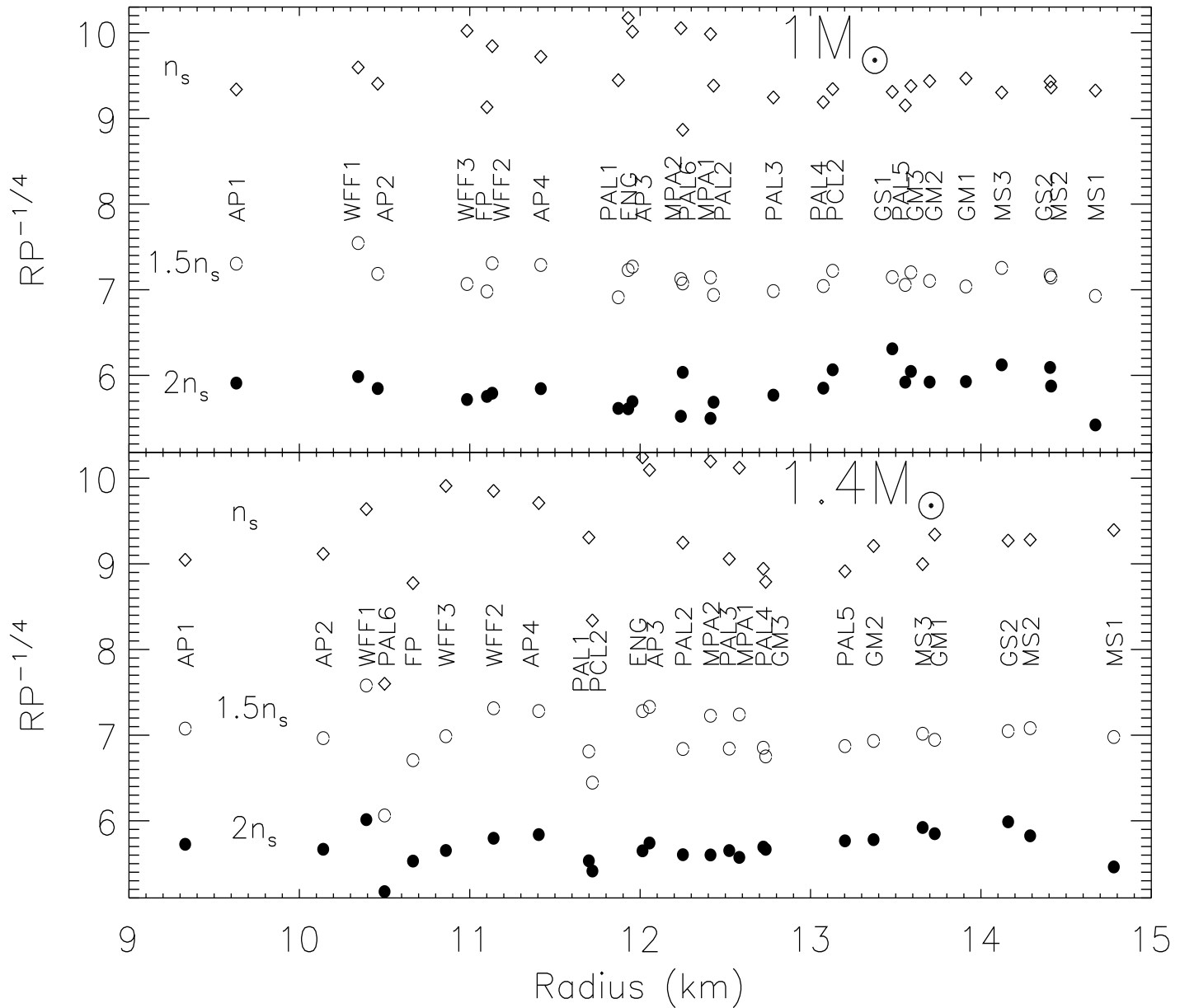
$$R \propto p_*^{1/4} \epsilon_*^{-1/2}$$

$$p_* = n^2 \frac{dE_{sym}}{dn} = \frac{n^2 L}{3n_s}$$



The Radius – Pressure Correlation

$$R \propto p^{1/4}$$



Lattimer & Prakash (2001)

Potentially Observable Quantities

- Apparent angular diameter from flux and temperature measurements

$$\beta \equiv GM/Rc^2$$

$$\frac{R_\infty}{D} = \frac{R}{D} \frac{1}{\sqrt{1-2\beta}} = \sqrt{\frac{F_\infty}{\sigma}} \frac{1}{f_\infty^2 T_\infty^2}$$

- Redshift

$$z = (1 - 2\beta)^{-1/2} - 1$$

- Eddington flux

$$F_{EDD} = \frac{GMc}{\kappa c^2 D^2} (1 - 2\beta)^{1/2}$$

- Crust thickness $(\ln \mathcal{H} = (2/m_b c^2) \int_0^{p_t} (dp/n))$

$$\frac{\Delta}{R} \equiv \frac{R - R_t}{R} = \frac{(\mathcal{H} - 1)(1 - 2\beta)}{\mathcal{H} + 2\beta - 1} \simeq (\mathcal{H} - 1) \left(\frac{1}{2\beta} - 1 \right).$$

- Moment of Inertia

$$I \simeq (0.237 \pm 0.008) MR^2 (1 + 2.84\beta + 18.9\beta^4) M_\odot \text{ km}^2$$

- Crustal Moment of Inertia

$$\frac{\Delta I}{I} \simeq \frac{8\pi}{3} \frac{R^6 p_t}{IMc^2}$$

- Binding Energy

$$\text{B.E.} = \frac{N - M}{M} \simeq (0.60 \pm 0.05) \frac{\beta}{1 - \beta/2}$$

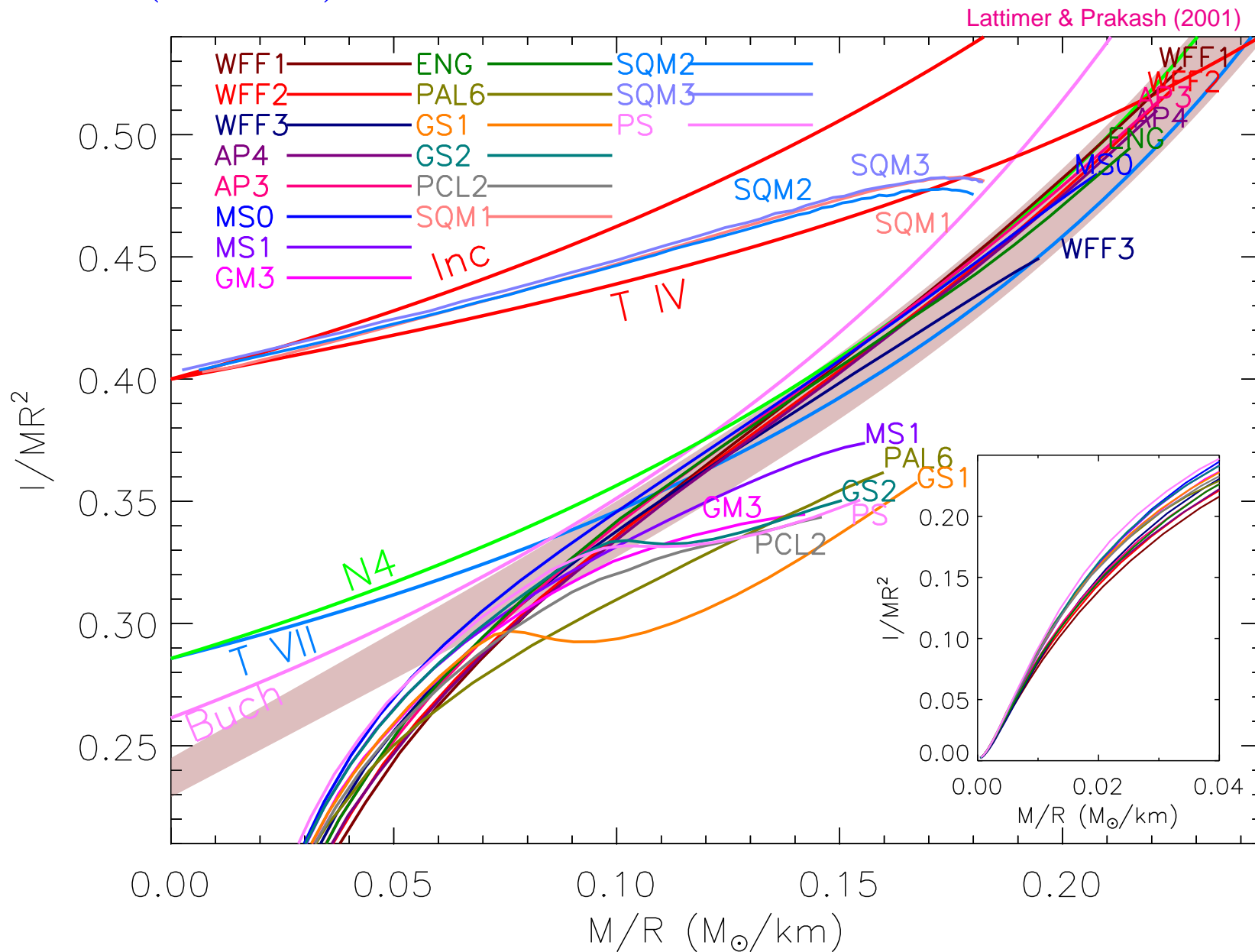
- Tidal Love Number

$$Q_{ij} = -\lambda E_{ij}, \quad \lambda = (2/3G)k_2 R^5$$

Moment of Inertia

- Spin-orbit coupling of same magnitude as post-post-Newtonian effects (Barker & O'Connell 1975, Damour & Schaeffer 1988)
- Precession alters inclination angle and periastron advance
- More EOS sensitive than R : $I \propto MR^2$
- Requires extremely relativistic system to extract
- Double pulsar PSR J0737-3037 is a marginal candidate
- Even more relativistic systems should be found, based on dimness and nearness of PSR J0737-3037

$I(M, R)$



$$I \simeq (0.237 \pm 0.008) MR^2 \left[1 + 4.2 \frac{M \text{ km}}{R M_\odot} + 90 \left(\frac{M \text{ km}}{R M_\odot} \right)^4 \right]$$

Moments of Inertia and Precession

- Spin-orbit coupling: $\dot{\vec{S}}_A = -\dot{\vec{L}} = \frac{G(4M_A+3M_B)}{2M_A a^3 c^2} \vec{L} \times \vec{S}_A$

Moments of Inertia and Precession

- Spin-orbit coupling: $\dot{\vec{S}}_A = -\dot{\vec{L}} = \frac{G(4M_A+3M_B)}{2M_A a^3 c^2} \vec{L} \times \vec{S}_A$
- Precession Period:

$$P_p = \frac{2(M_A + M_B)ac^2}{GM_B(4M_A + 3M_B)} P(1 - e^2) \simeq 74.9 \text{ years}$$

Moments of Inertia and Precession

- Spin-orbit coupling: $\dot{\vec{S}}_A = -\dot{\vec{L}} = \frac{G(4M_A+3M_B)}{2M_A a^3 c^2} \vec{L} \times \vec{S}_A$
- Precession Period:

$$P_p = \frac{2(M_A + M_B)ac^2}{GM_B(4M_A + 3M_B)} P(1 - e^2) \simeq 74.9 \text{ years}$$

- Precession Amplitude $\propto \vec{S}_A \times \vec{L}$:

$$\delta_i = \frac{|\vec{S}_A|}{|\vec{L}|} \sin \theta \simeq \frac{I_A(M_A + M_B)}{a^2 M_A M_B} \frac{P}{P_A} \sin \theta \simeq (3.6 - 7.2) \sin \theta \times 10^{-5}$$

Moments of Inertia and Precession

- Spin-orbit coupling: $\dot{\vec{S}}_A = -\dot{\vec{L}} = \frac{G(4M_A+3M_B)}{2M_A a^3 c^2} \vec{L} \times \vec{S}_A$
- Precession Period:

$$P_p = \frac{2(M_A + M_B)ac^2}{GM_B(4M_A + 3M_B)} P(1 - e^2) \simeq 74.9 \text{ years}$$

- Precession Amplitude $\propto \vec{S}_A \times \vec{L}$:

$$\delta_i = \frac{|\vec{S}_A|}{|\vec{L}|} \sin \theta \simeq \frac{I_A(M_A + M_B)}{a^2 M_A M_B} \frac{P}{P_A} \sin \theta \simeq (3.6 - 7.2) \sin \theta \times 10^{-5}$$

- Delay in Time-of-Arrival:

$$\delta t_a = \left(\frac{M_B}{M_A + M_B} \right) \frac{a}{c} \delta_i \cos i \approx 0.4 - 4.0 \sin \theta \mu\text{s}$$

Moments of Inertia and Precession

- Spin-orbit coupling: $\dot{\vec{S}}_A = -\dot{\vec{L}} = \frac{G(4M_A+3M_B)}{2M_A a^3 c^2} \vec{L} \times \vec{S}_A$
- Precession Period:

$$P_p = \frac{2(M_A + M_B)ac^2}{GM_B(4M_A + 3M_B)} P(1 - e^2) \simeq 74.9 \text{ years}$$

- Precession Amplitude $\propto \vec{S}_A \times \vec{L}$:

$$\delta_i = \frac{|\vec{S}_A|}{|\vec{L}|} \sin \theta \simeq \frac{I_A(M_A + M_B)}{a^2 M_A M_B} \frac{P}{P_A} \sin \theta \simeq (3.6 - 7.2) \sin \theta \times 10^{-5}$$

- Delay in Time-of-Arrival:

$$\delta t_a = \left(\frac{M_B}{M_A + M_B} \right) \frac{a}{c} \delta_i \cos i \approx 0.4 - 4.0 \sin \theta \mu\text{s}$$

- Periastron Advance $\propto \vec{S}_A \cdot \vec{L}$: $A_P/A_{PN} =$

$$\frac{2\pi I_A}{P_A} \left(\frac{2 + 3M_B/M_A}{3M_A^2 + 3M_B^2 + 2M_A M_B} \right) \sqrt{\frac{M_A + M_B}{Ga}} \cos \theta \simeq (2.2 - 4.3) \times 10^{-4} \cos \theta$$

Moments of Inertia and Precession

- Spin-orbit coupling: $\dot{\vec{S}}_A = -\dot{\vec{L}} = \frac{G(4M_A+3M_B)}{2M_A a^3 c^2} \vec{L} \times \vec{S}_A$
- Precession Period:

$$P_p = \frac{2(M_A + M_B)ac^2}{GM_B(4M_A + 3M_B)} P(1 - e^2) \simeq 74.9 \text{ years}$$

- Precession Amplitude $\propto \vec{S}_A \times \vec{L}$:

$$\delta_i = \frac{|\vec{S}_A|}{|\vec{L}|} \sin \theta \simeq \frac{I_A(M_A + M_B)}{a^2 M_A M_B} \frac{P}{P_A} \sin \theta \simeq (3.6 - 7.2) \sin \theta \times 10^{-5}$$

- Delay in Time-of-Arrival:

$$\delta t_a = \left(\frac{M_B}{M_A + M_B} \right) \frac{a}{c} \delta_i \cos i \approx 0.4 - 4.0 \sin \theta \mu\text{s}$$

- Periastron Advance $\propto \vec{S}_A \cdot \vec{L}$: $A_P/A_{PN} =$

$$\frac{2\pi I_A}{P_A} \left(\frac{2 + 3M_B/M_A}{3M_A^2 + 3M_B^2 + 2M_A M_B} \right) \sqrt{\frac{M_A + M_B}{Ga}} \cos \theta \simeq (2.2 - 4.3) \times 10^{-4} \cos \theta$$

- Moment of Inertia – Mass – Radius

$$I \simeq (0.237 \pm 0.008) M R^2 \left[1 + 4.2 \frac{M \text{ km}}{R M_\odot} + 90 \left(\frac{M \text{ km}}{R M_\odot} \right)^4 \right]$$

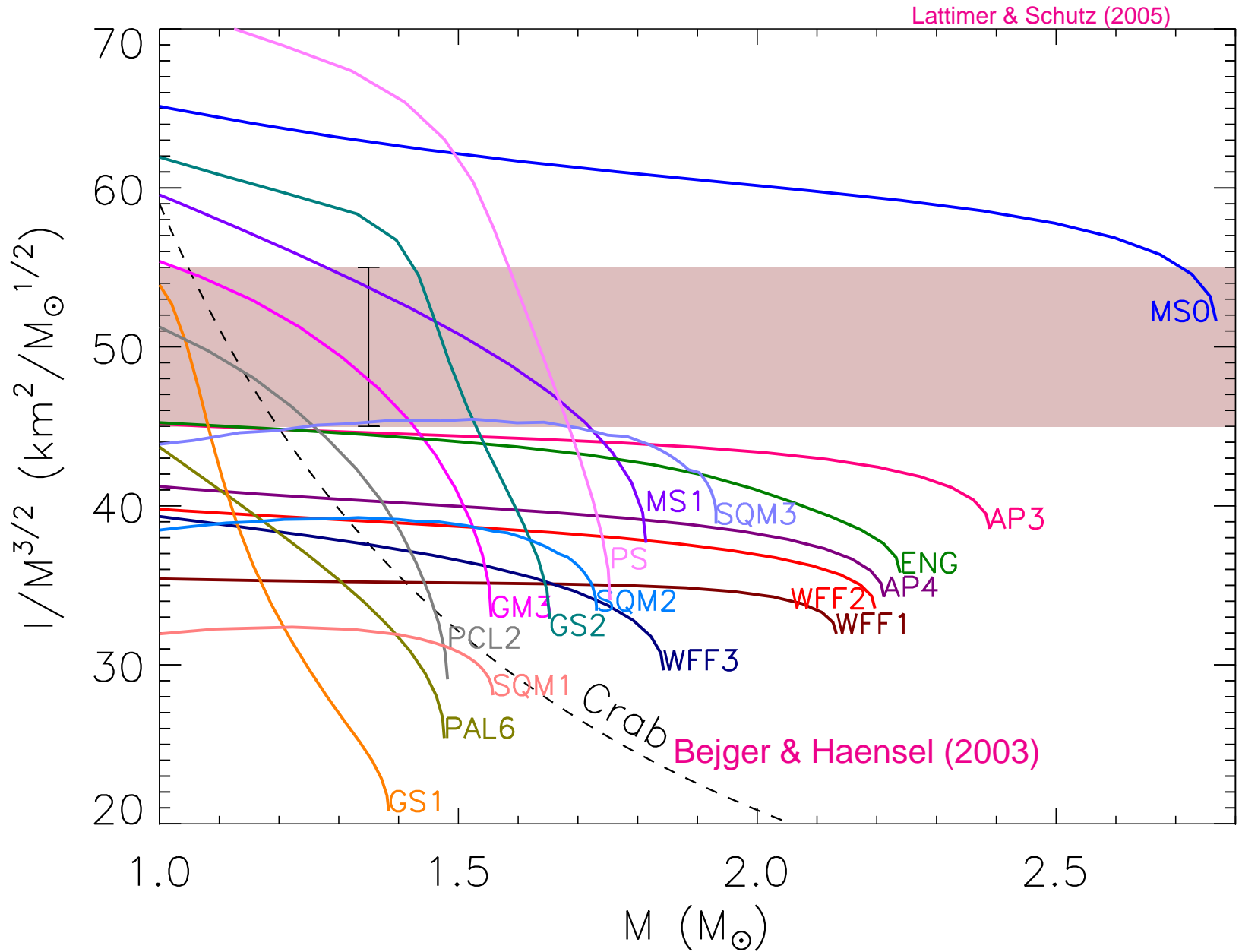
Comparison of Binary Pulsars

References	PSR 0707-3039 a, b, c	PSR 1913+16 d	PSR 1534+12 e, f
a/c (s)	2.93	6.38	7.62
P (h)	2.45	7.75	10.1
e	0.088	0.617	0.274
M_A (M_\odot)	1.337 ± 0.005	1.4414 ± 0.0002	1.333 ± 0.001
M_B (M_\odot)	1.250 ± 0.005	1.3867 ± 0.0002	1.345 ± 0.001
T_{GW} (M yr)	85	245	2250
i	$87.9 \pm 0.6^\circ$	47.2°	77.2°
P_A (ms)	22.7	59	37.9
θ_A	$13^\circ \pm 10^\circ$	21.1°	$25.0^\circ \pm 3.8^\circ$
ϕ_A	$246^\circ \pm 5^\circ$	9.7°	$290^\circ \pm 20^\circ$
P_{pA} (yr)	74.9	297.2	700
$\delta t_a / I_{A,80}$ (μs)	0.7 ± 0.6	11.2	7.9 ± 1.1
$A_{pA} / (A_{1PN} I_{A,80})$	$3.4^{+0.2}_{-0.1} \times 10^{-5}$	1.0×10^{-5}	$1.15^{+0.04}_{-0.03} \times 10^{-5}$
A_{2PN} / A_{1PN}	5.2×10^{-5}	4.7×10^{-5}	2.3×10^{-5}

a: Lyne et al. (2004); b: Solution 1, Jenet & Ransom (2004); c: Coles et al. (2004)

d: Weisberg & Taylor (2002, 2004); e: Stairs et al. (2002, 2004); f: Bogdanov et al. (2002)

EOS Constraint



Tidal Effects in Mergers

Thesis work of Sergey Postnikov (Ohio University) in collaboration with M. Praksh and JML

- Masses of components of inspiralling neutron stars will be well measured.
- Large finite-size effects like mass exchange and tidal disruption will be visible in the gravitational wave signal toward the end of inspiral
- However, the gravitational wave signal is very complex during this period
- Tidal effects are potentially measurable during the earlier part of the evolution when the waveform is relatively clean; it is a cumulative effect
- The effect depends on the induced quadrupole moment Q_{ij} , which is proportional to the applied tidal field E_{ij}
- In early evolution, tidal effects form a very small correction in which the accumulated phase shift is characterized by the weighted average Q_{ij} for the two stars.
- The proportionality constant depends on the stellar radius and the internal structure: $\lambda = (2/3G)k_2R^5$
- The tidal Love number k_2 depends on the equation of state and compactness β
- Pronounced differences in k_2 exist between neutron stars and strange quark stars
- The extreme dependence on R offers a possibility of a constraint

Computation of Tidal Love Numbers

We follow Thorne & Campolattaro (1967 ApJ 149, 591) and Hinderer (2008 ApJ 677, 1216):

$$\begin{aligned} k_2(\beta, y_R) &= \frac{8}{5} \beta^5 (1 - 2\beta)^2 [2 - y_R + 2\beta(y_R - 1)] \times \\ &\times \{2\beta (6 - 3y_R + 3\beta(5y_R - 8)) + 2\beta^2 [13 - 11y_R + \beta(3y_R - 2) + 2\beta^2(1 + y_R)] \\ &+ 3(1 - 2\beta)^2 [2 - y_R + 2\beta(y_R - 1)] \ln(1 - 2\beta)\}^{-1}. \end{aligned}$$

$$y_R = [rH'(r)/H(r)]_{r=R}$$

$$\begin{aligned} H''(r) + H'(r) \left[\frac{2}{r} + e^{\lambda(r)} \left(\frac{2m(r)}{r^2} + 4\pi r[p(r) - \rho(r)] \right) \right] + H(r)Q(r) &= 0, \\ Q(r) &= 4\pi e^{\lambda(r)} \left(5\rho(r) + 9p(r) + \frac{\rho(r) + p(r)}{c_s^2(r)} \right) - 6 \frac{e^{\lambda(r)}}{r^2} - (\nu'(r))^2. \end{aligned}$$

Can be simplified:

$$\begin{aligned} ry'(r) + y(r)^2 + y(r)e^{\lambda(r)} (1 + 4\pi r^2[p(r) - \rho(r)]) + r^2Q(r) &= 0, \\ y(0) &= 2 \end{aligned}$$

Newtonian Limit

$$p \ll \rho, \quad \rho r^2 \ll 1$$

$$k_2(y_R) = \frac{1}{2} \frac{2 - y_R}{3 + y_R},$$

$$r y'(r) + y(r)^2 + y(r) - 6 + 4\pi r^2 \frac{\rho(r)}{c_s^2(r)} = 0.$$

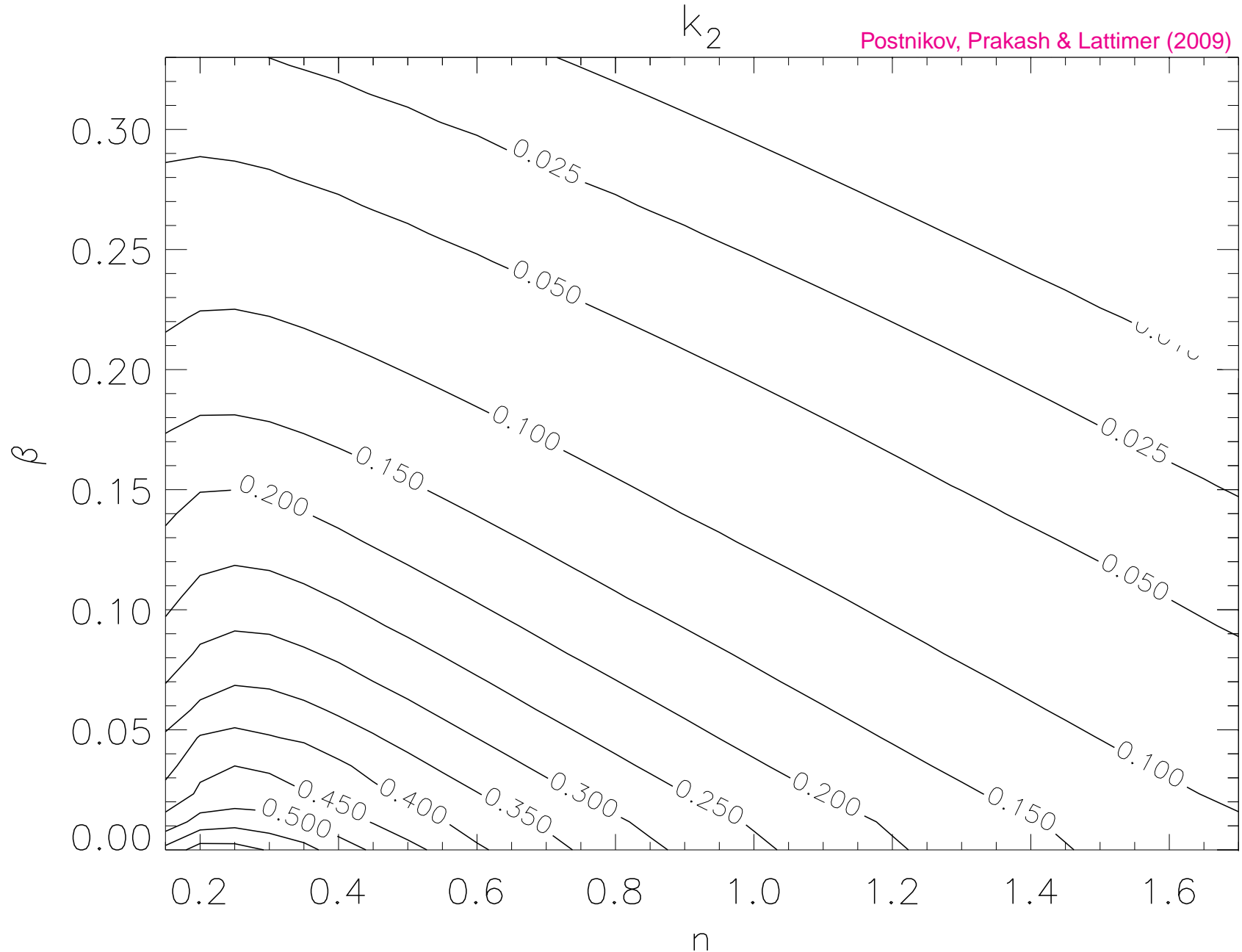
Analytic polytropic cases:

$$n = 0 : \quad y(r) = 2, \quad k_2 = 0$$

But Damour & Nagar (archiv:0906.0096) claim that the density discontinuity at the surface changes this such that $y_R = -1$ and $k_2 = 3/4$.

$$n = 1 : \quad y(r) = \frac{\pi r}{R} \frac{J_{3/2}(\pi r/R)}{J_{5/2}(\pi r/R)} - 3, \quad y_R = \frac{\pi^2 - 9}{3}, \quad k_2 = \frac{15 - \pi^2}{2\pi^2}$$

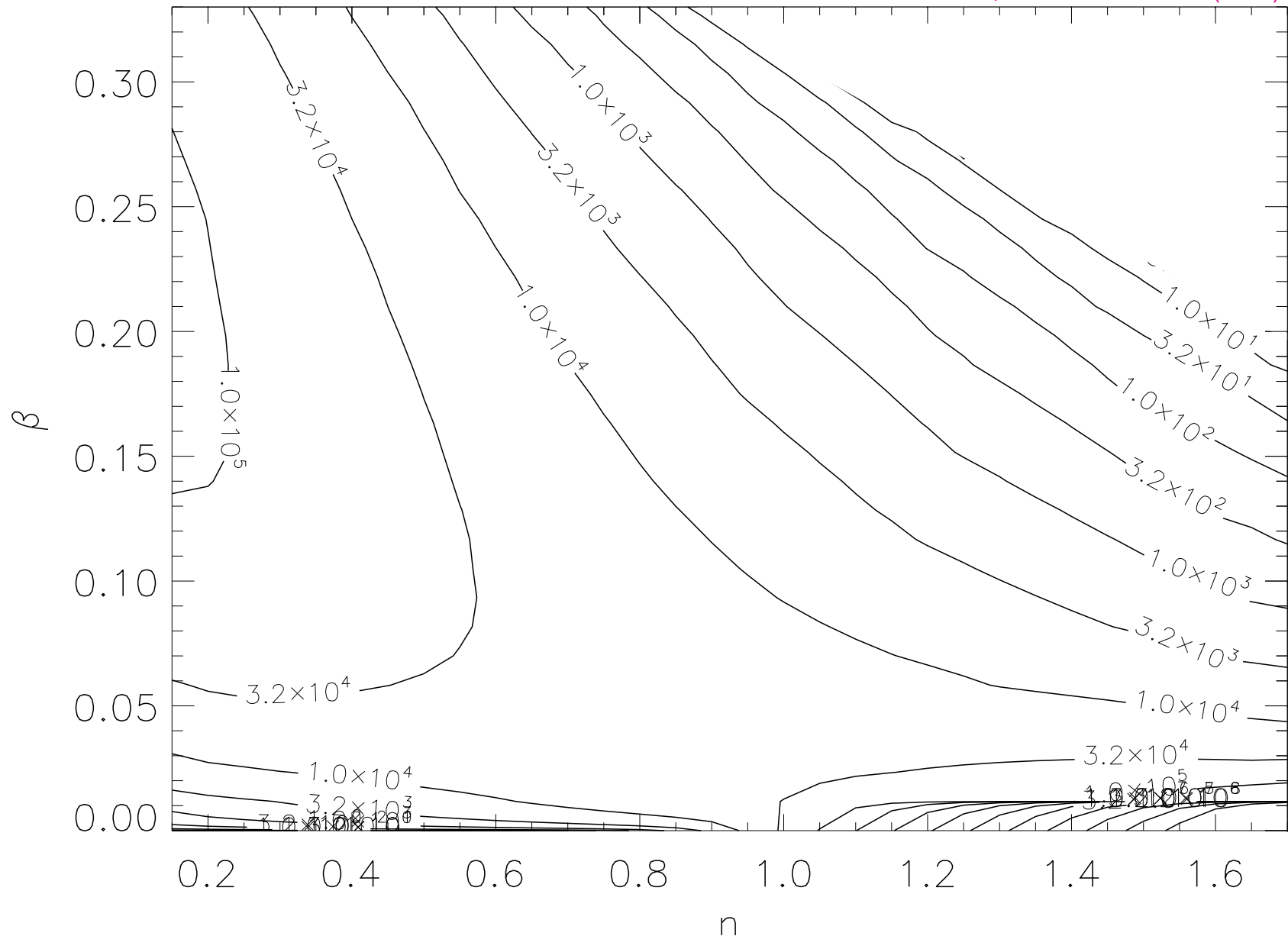
Tidal Love Numbers of Polytropes



Tidal Love Numbers of Polytropes

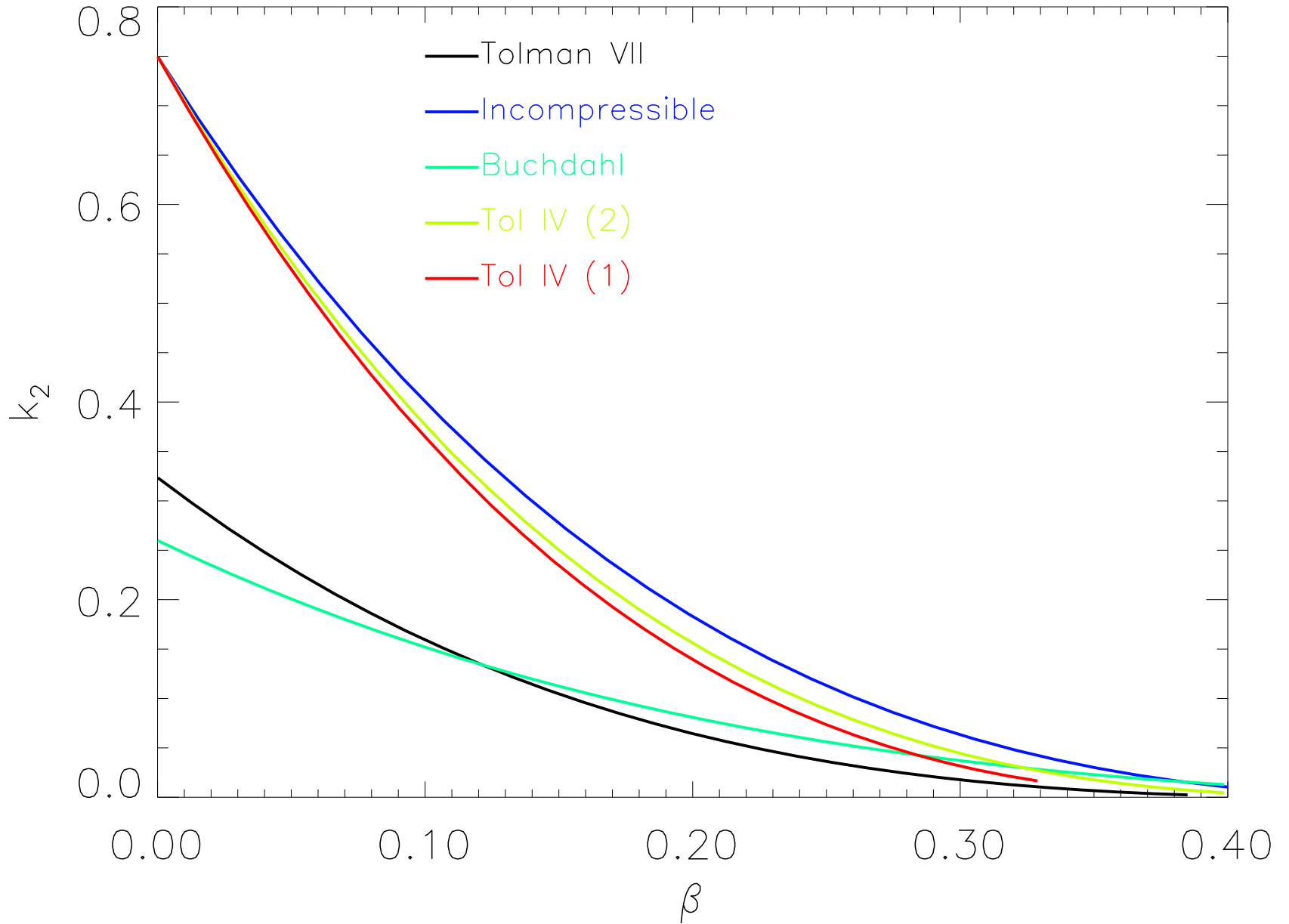
λ (km^5)

Postnikov, Prakash & Lattimer (2009)



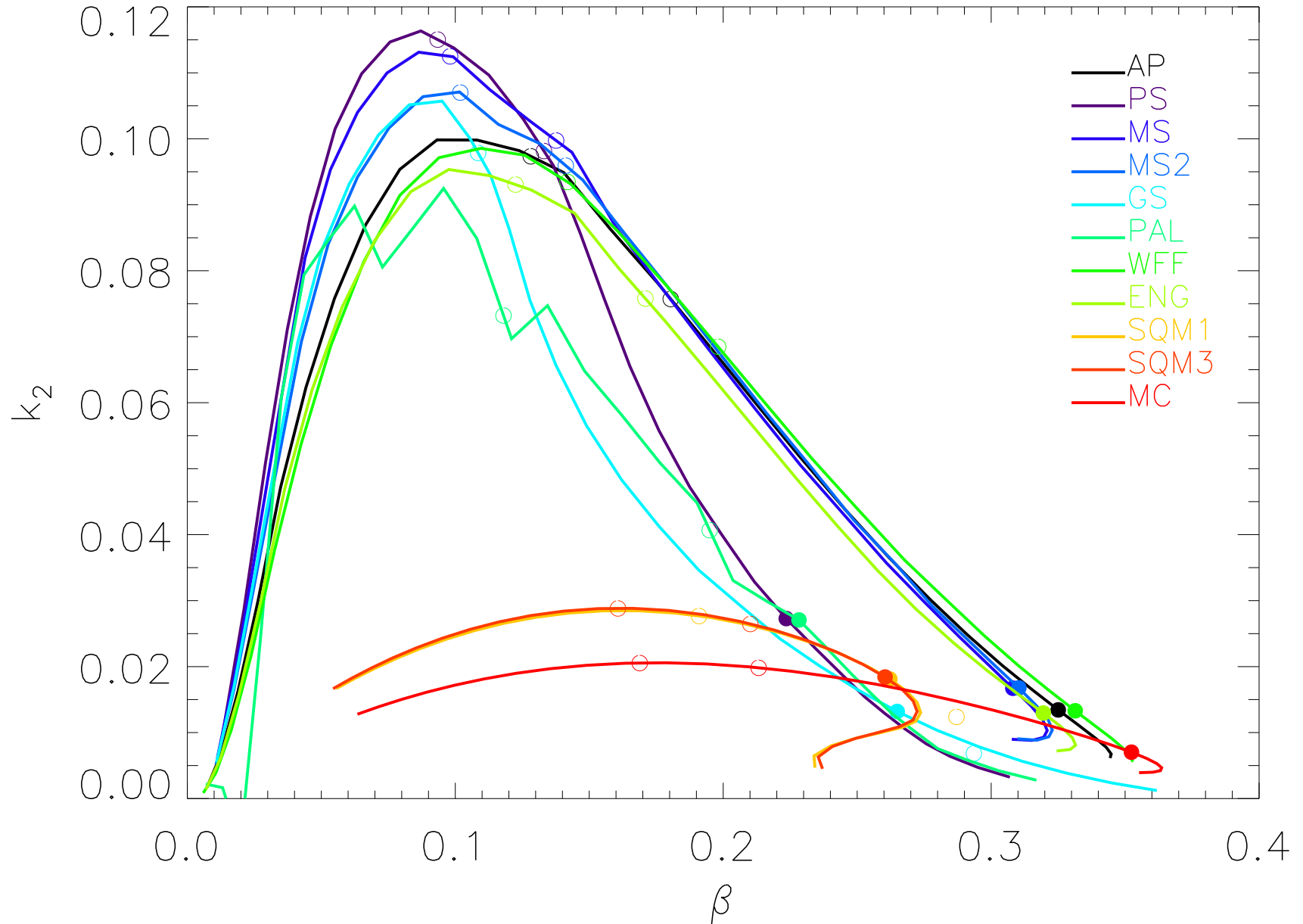
Tidal Love Numbers of Analytic Solutions

Postnikov, Prakash & Lattimer (2009)



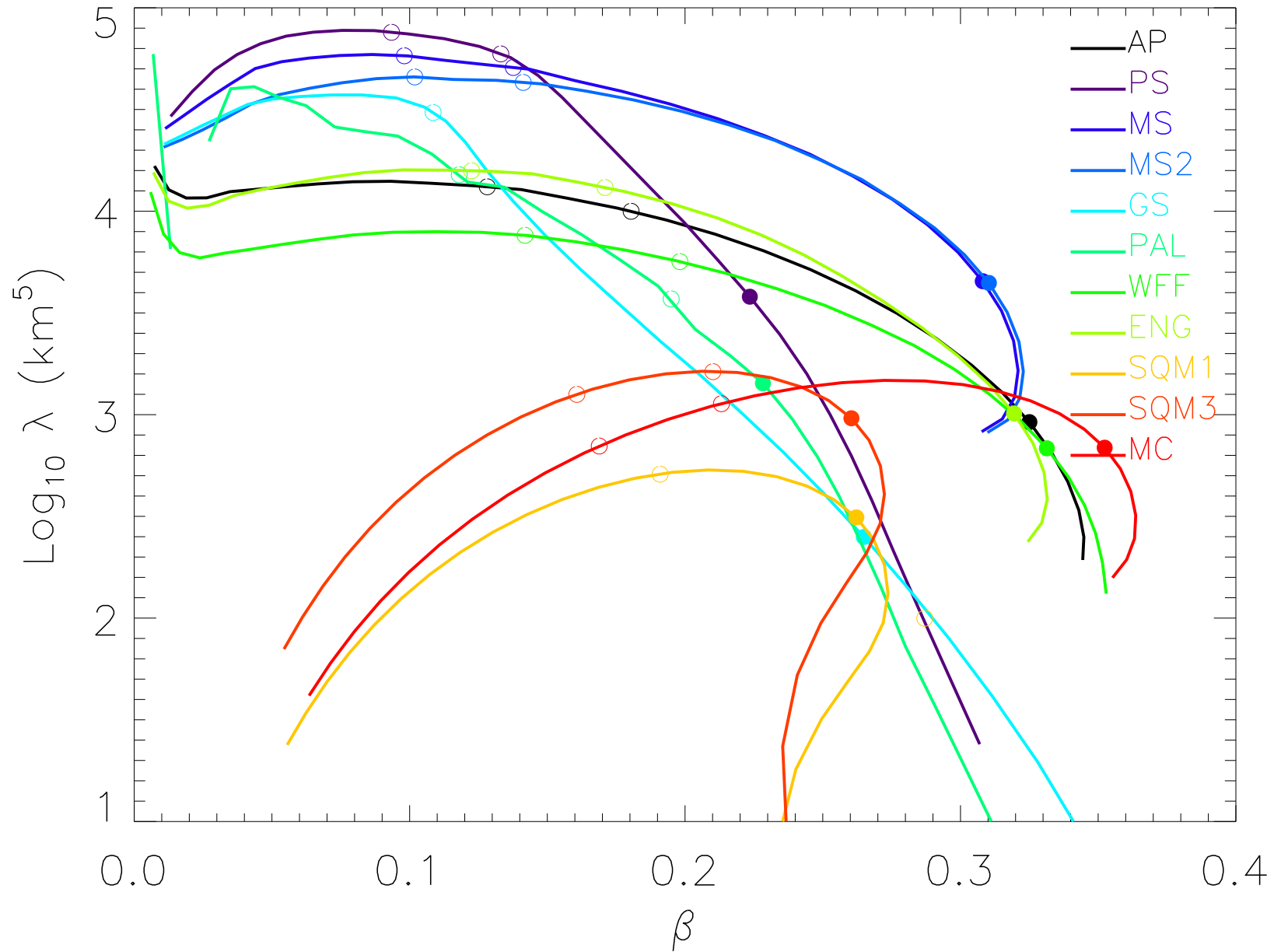
Tidal Love Numbers of Realistic Equations of State

Postnikov, Prakash & Lattimer (2009)



Tidal Love Numbers of Realistic Equations of State

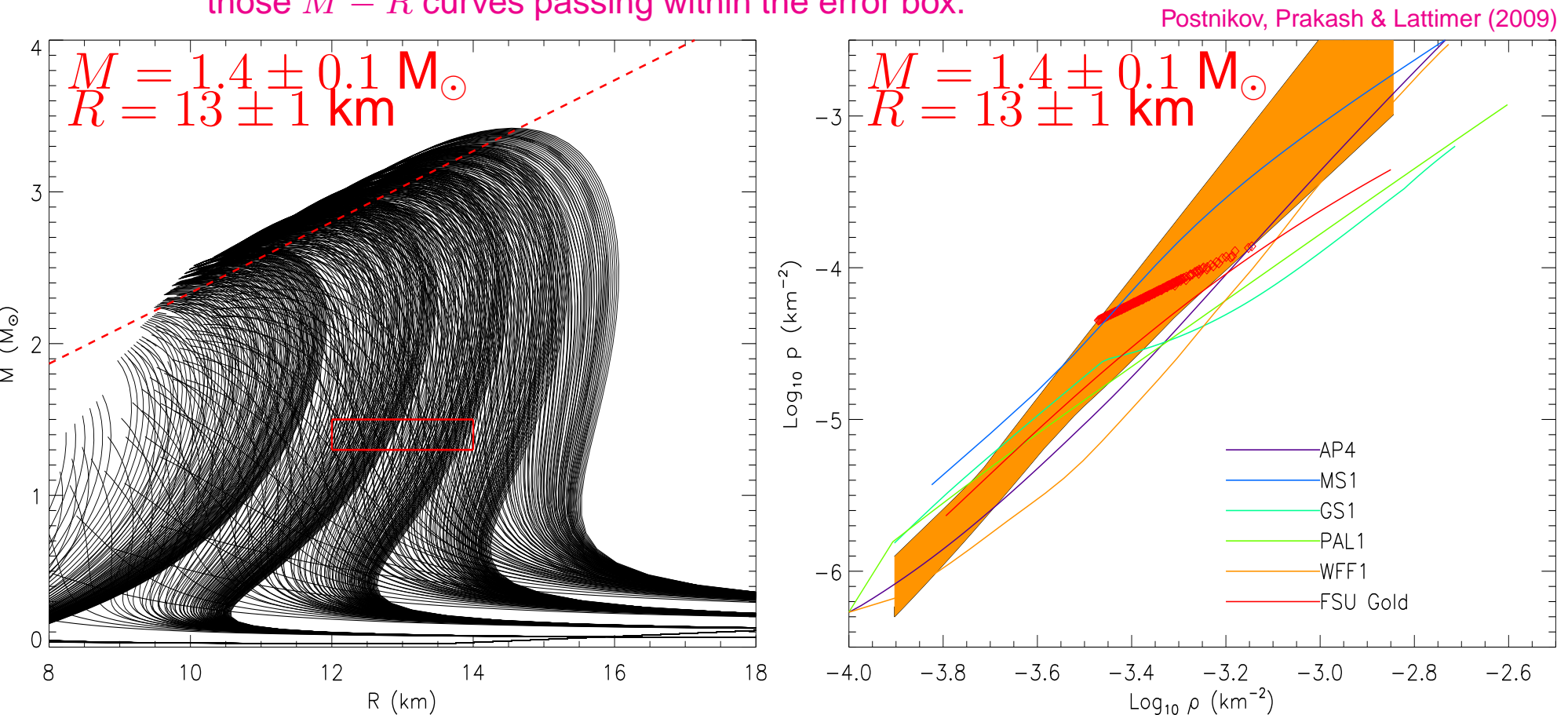
Postnikov, Prakash & Lattimer (2009)



TOV Inversion

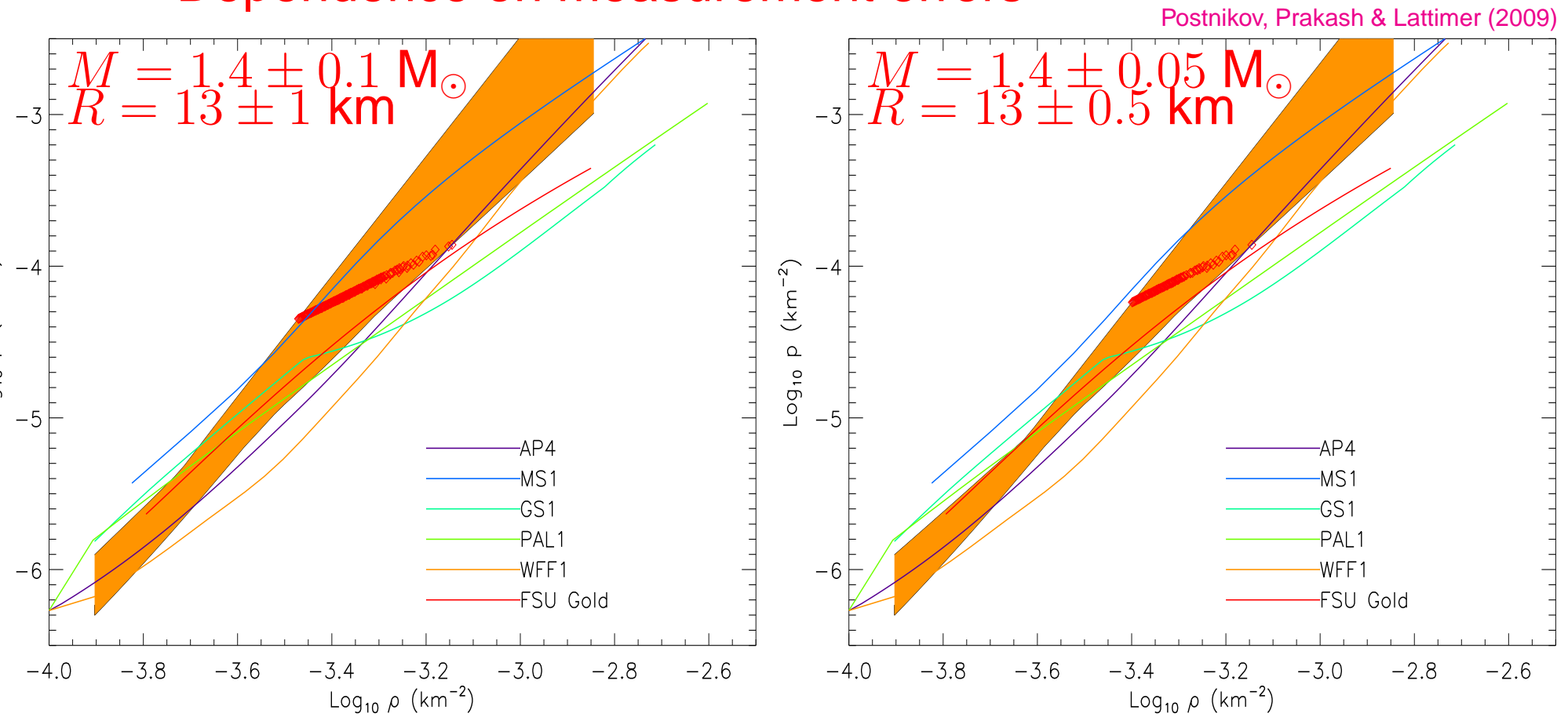
How would a simultaneous $M - R$ determination constrain the EOS? Each $M - R$ curve specifies a unique $p - \rho$ relation.

- Generate physically reasonable $M - R$ curves and the $p - \rho$ relations that they specify.
- Generate arbitrary $p - \rho$ relations and compute $M - R$ curves from them; select those $M - R$ curves passing within the error box.



TOV Inversion (cont.)

Dependence on measurement errors



The current uncertainty in the subnuclear EOS introduces significant width to the inferred high-density pressure-density relation.

Conclusions

- Neutron stars are a powerful laboratory to constrain dense matter physics, especially the symmetry energy and composition at supranuclear densities.
- Many aspects of neutron star structure depend on specific equation of state parameters or their density dependence in a model-independent fashion.
- Increasing evidence supports the existence of massive neutron stars ($M \gtrsim 1.7 M_{\odot}$), constraining exotic matter.
- Many kinds of observations are now available to constrain neutron star radii, although no reliable measures yet exist.
- An accurate, simultaneous mass and radius measurement from even one neutron star would provide a significant constraint.